Let your fingers do the walking: a simple spectral signature model for “remote” fossil prospecting.

By: Glenn C. Conroy, Charles W. Emerson, Robert L. Anemone, and K.E. Beth Townsend

GC Conroy, CW Emerson, RL Anemone, KEB Townsend (2012) Let your fingers do the walking: a simple spectral signature model for “remote” fossil prospecting. *Journal of Human Evolution*, 63(1): 79-84.

Abstract:

Even with the most meticulous planning, and utilizing the most experienced fossil-hunters, fossil prospecting in remote and/or extensive areas can be time-consuming, expensive, logistically challenging, and often hit or miss. While nothing can predict or guarantee with 100% assurance that fossils will be found in any particular location, any procedures or techniques that might increase the odds of success would be a major benefit to the field. Here we describe, and test, one such technique that we feel has great potential for increasing the probability of finding fossiliferous sediments - a relatively simple spectral signature model using the spatial analysis and image classification functions of ArcGIS®10 that creates interactive thematic land cover maps that can be used for “remote” fossil prospecting. Our test case is the extensive Eocene sediments of the Uinta Basin, Utah – a fossil prospecting area encompassing ~1200 square kilometers. Using Landsat 7 ETM+ satellite imagery, we “trained” the spatial analysis and image classification algorithms using the spectral signatures of known fossil localities discovered in the Uinta Basin prior to 2005 and then created interactive probability models highlighting other regions in the Basin having a high probability of containing fossiliferous sediments based on their spectral signatures. A fortuitous “post-hoc” validation of our model presented itself. Our model identified several paleontological “hotspots”, regions that, while not producing any fossil localities prior to 2005, had high probabilities of being fossiliferous based on the similarities of their spectral signatures to those of previously known fossil localities. Subsequent fieldwork found fossils in all the regions predicted by the model.

Keywords: human evolution | fossil prospecting | remote sensing | geographic information systems | image classification | uinta basin | archaeology | anthropology

Article:

Introduction

Archeologists have long recognized the value of geospatial technologies for site discovery and analyses, including (among others) prospecting for new sites, developing predictive models for site location, and spatial analysis of artifacts within a single site (Carr and Turner, 1996; Kvamme, 1999; Ostir et al., 1999; Mehrer and Westcott, 2006; McCoy and Ladefoged, 2009; Parcak, 2009; Giardino, 2011). We have recently reviewed how Remote Sensing (RS) and Geographic Information Systems (GIS) have been, and are being, used in paleoanthropology and related disciplines to great advantage (Conroy, 2006; Conroy et al., 2008; Anemone et al., 2011a). We have also shown how artificial neural network (ANN) models can be developed to aid in fossil prospecting (Anemone et al., 2011b; Emerson and Anemone, 2012). Here we expand on our previous work by describing, and testing, a relatively simple spectral signature model derived from Landsat ETM+ satellite imagery using the spatial analysis and image classification functions of ArcGIS®10 to create interactive thematic land cover maps that can be used for "remote" fossil prospecting in the vast expanses of the Uinta Basin, Utah. The image classification process involves conversion of multi-band Landsat ETM+ raster imagery into single-band probability rasters with a number of categorical classes that relate to different land cover types – one of which is the "probability" of spectral similarity to localities that were previously shown to be fossiliferous.

Uinta Basin: paleontological and geological overview

Before describing our classification model, we provide here a brief overview of the study area in which we developed and tested the model.

The Uinta Formation (~1298 m thick including subsurface and exposed rock) overlies the lacustrine Green River Formation and is exposed along the southern base of the Uinta Mountains. It can be traced westward as far as Duchesne near the Wasatch Mountain Range and as far eastward as the Utah-Colorado state line (Peterson and Kay, 1931; Bryant et al., 1989; Hamblin et al., 1999) (Fig. 1). The Uinta Formation was deposited under fluvial conditions as the lake depositing the Green River Formation was receding (Ryder et al., 1976).

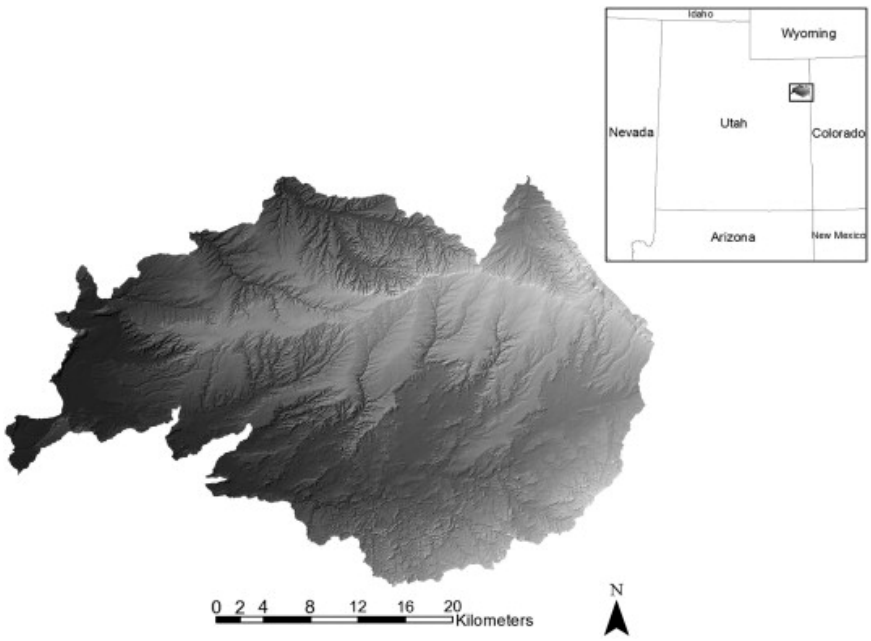

Figure 1.

Digital Elevation Model (DEM) of the Uinta Basin and its location along the Utah/Colorado border.

O.C. Marsh led the first paleontological expedition to the Uinta basin in 1870 and collected numerous fossil mammals between the Green and White rivers (Betts, 1871; Marsh, 1875a, b). This fossil assemblage would later define the Uintan North American Land Mammal Age (NALMA), a time period that spans ~40–46.5 Ma (Wood et al., 1941; Prothero, 1996). Collecting continued in the 1880s by Francis Speir of Princeton University. These fossils were studied by W.B. Scott and H.F. Osborn, who produced the first comprehensive publications on Uintan mammals (Scott and Osborn, 1887, 1890). In the early 1900's, O.A. Peterson and later Earl Douglass from the Carnegie Museum sent expeditions to the Uinta basin and many of the medium and smaller-sized mammals from the Uinta Formation discovered during those expeditions became index taxa for the Uintan NALMA (Douglass, 1914; Peterson, 1919; Walsh, 1996). In 1993, expeditions initially from Washington University in St. Louis under the direction of D.T. Rasmussen, and after 2005 under the direction of one of us (KBT), began fossil prospecting in the Uinta and Duchesne River Formations (Rasmussen et al., 1999; Townsend, 2004; Townsend et al., 2006). These expeditions have amassed one of the largest assemblages of Uintan mammals from the Rocky Mountain region and the fossil localities discovered during these expeditions form the basic “fossil locality” data for this study. These fossil localities range over an extensive geographic area of ~1200 square kilometers (Figure 1 and Figure 3).

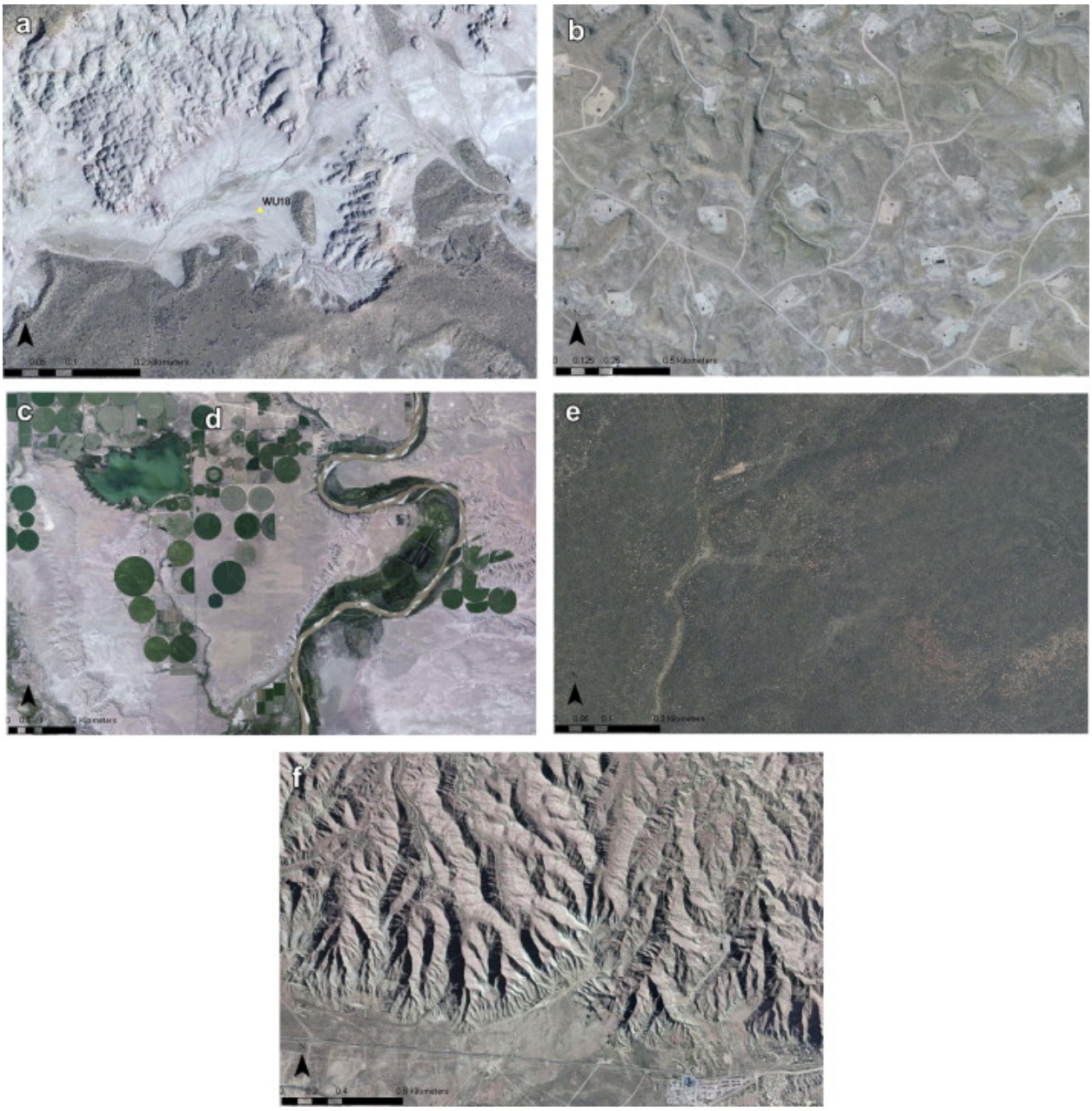

Figure 2.

Land cover classes of the Uinta Basin. (a) fossil localities, (b) oil/gas field infrastructure (graded well pads, access roads, pipelines, etc.); (c) water and (d) agriculture, e) scrub/tree cover, f) steep slopes.

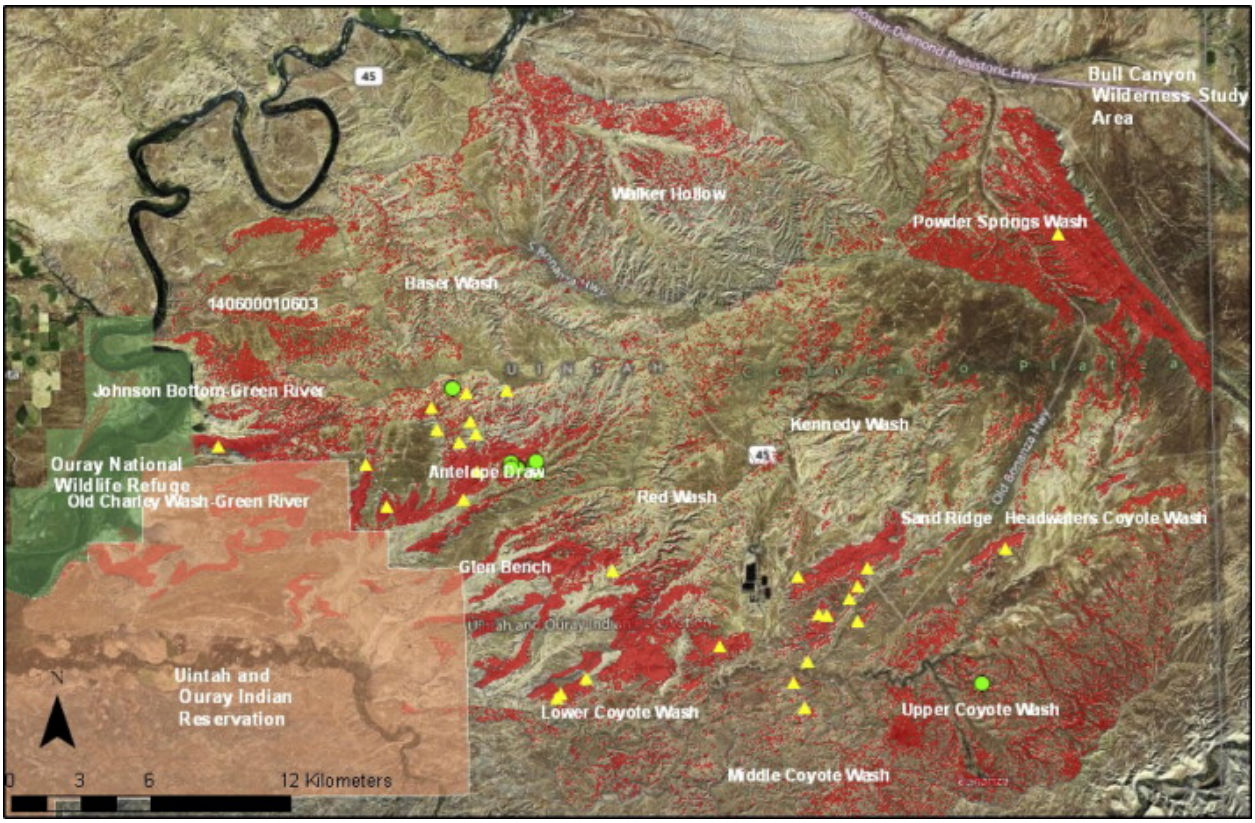

Figure 3.

Class probability map showing (in red) those cells (pixels) having both a >98% probability of falling within the land cover class “fossil localities” based on their spectral signatures and being mapped as Eocene on the geologic maps of Utah. Yellow triangles are Washington University (WU) fossil localities discovered prior to 2005. These are the fossil localities that the image classification program was “trained” on to identify the land cover class “fossil localities”. Green dots represent fossil localities discovered since 2005 and thus were not part of the original model training. Note that in all cases these fossil-bearing localities fall within areas predicted by our model. Our model identified a number of potentially rich fossiliferous areas to the west of Antelope Draw and Glen Bench. Unfortunately these areas are not open to paleontological collecting at this time, being located in either the Ouray National Wildlife Refuge or Uintah and Ouray Indian Reservation. A number of fossil vertebrate localities are, however, known to exist in these areas as our model predicts they should. (For interpretation of the references to color in this figure legend, the reader is referred to the web version of this article.)

The Uinta Formation is formally divided into a lower Wagonhound Member and an upper Myton Member; however, many geologists and paleontologists continue to utilize the informal tripartite scheme in which the formation is subdivided from lowest to highest into Uinta A, B and C. Uinta A is comprised of resistant, fine-grained sandstones that intertongue with the underlying Parachute Creek Member of the Green River Formation. Uinta B is composed of mudstones and

claystones forming non-resistant slopes that are interbedded with fine-grained sandstones forming thin resistant ledges. The lower part of Uinta C is comprised of mudstone and claystone interbedded with fine-grain sandstone beds, whereas the upper part is composed mainly of mudstone and claystone with thin fine-grain sandstone beds forming thin ledges (Townsend et al., 2006; Sprinkel, 2007; Murphey et al., 2011).

During the early Eocene, global climates were exceedingly warm and produced an almost pole-to-pole tropical greenhouse (Zachos et al., 2001). The Uintan NALMA, and the final intervals of the preceding Bridgerian NALMA, mark the beginning of the end of this global greenhouse, and this is reflected in the ecological diversity of the mammals that lived during this time (Woodburne et al., 2009; Townsend et al., 2010). Tropical arboreal forms typical of the early Eocene greenhouse began to disappear, and mammals that were more adapted to subtropical, even temperate conditions and habitats, made their first appearances. The Uintan NALMA also marks a key transition in the evolutionary history of North American mammalian faunas – a time when ~31% of modern mammalian families first appear in the fossil record including the ancestors of modern canids, camelids, felids, and some modern rodents (Black and Dawson, 1966).

Materials and methods

Spectral signature model

Landsat 7 ETM+ satellite data for the Uinta Basin from July 7, 2002 was downloaded from the Landsat Archives 1999–2003 collection (Path/Row 36, 32) available at USGS Global Visualization Viewer (http://glovis.usgs.gov/), unzipped (using 7-Zip), and then imported into ArcGIS®10. Satellite bands 1–5 and 7 (see Table 1) were compiled (band 6 is the thermal band, which tends to blur the class signatures (see below)). Using band 8, the Landsat ETM+ panchromatic band, the original 30 m visible and near- and mid-infrared bands were pan-enhanced to a spatial resolution of 15 m. We experimented with a number of different (R)ed, (G)reen, (B)lue band combinations and found that a RGB combination of bands 7, 5, 1 gave us the best visual contrasts for the various Uinta Basin land cover classes we were interested in (Fig. 2). Images created using different bands (or wavelengths) have different contrast (light and dark areas). Computers make it possible to assign “false color” to these black and white images. The three primary colors of light are red, green, and blue. Computer screens can display an image in three different bands at a time, by using a different primary color for each band. When these three images are combined (in our case, bands 7, 5, 1) a “false color image” is produced. Although the “false color image” is created using a combination of three bands, it is important to emphasize that the image classification procedure described below uses data from all bands.

Table 1.

Landsat 7 ETM+ band characteristics.

Band 1 (0.45–0.52 μm, blue-green): Since this short wavelength of light penetrates better than the other bands it is often the band of choice for aquatic ecosystems. It is used to monitor sediment in water, mapping coral reefs, and water depth. Unfortunately this is the noisiest of the Landsat bands since short wavelength blue light is scattered more than the other bands. For this reason it is rarely used for "pretty picture" type images. Ground Resolution 30 m
Band 2 (0.52–0.60 μm, green): This has similar qualities to band 1 but not as extreme. The band was selected because it matches the wavelength for the green we see when looking at vegetation. Ground Resolution 30 m
Band 3 (0.63–0.69 μm, red): Since vegetation absorbs nearly all red light (it is sometimes called the chlorophyll absorption band) this band can be useful for distinguishing between vegetation, soil, and roads, and in monitoring vegetation health. Ground Resolution 30 m
Band 4 (0.76–0.90 μm, near infrared): Since water absorbs nearly all light at this wavelength water bodies appear very dark. This contrasts with bright reflectance for soil and vegetation, so it is a good band for defining the water/land interface. Ground Resolution 30 m
Band 5 (1.55–1.75 μm, mid-infrared): This band is very sensitive to moisture and is therefore used to monitor vegetation and soil moisture. It is also good at differentiating between clouds and snow, and between roads, bare soils, and water. It has excellent atmospheric and haze penetration. Ground Resolution 30 m
Band 6 (10.40–12.50 μm, thermal infrared): This is a thermal band, which means it can be used to measure surface temperature. This is primarily used for geological applications but it is sometime used to measure plant heat stress. This is also used to differentiate clouds from bright soils since clouds tend to be very cold. One other difference between this band and the other multispectral ETM bands is that the resolution is 60 m instead of 30 m.
Band 7 (2.08–2.35 μm mid-infrared): This band is used to differentiate mineral and rock types and also for interpreting vegetation cover and soil moisture. Ground Resolution 30 m.
Band 8 (0.520–0.900 μm panchromatic band, black and white imagery): This band yields

enhanced resolution and increased detection ability.

*Source:*biodiversityinformatics.amnh.org.

There are two primary ways to classify a multi-band raster image; supervised and unsupervised classification. In the supervised classification method, the investigator classifies the image using spectral signatures (i.e., reflectance values) obtained from training samples (polygons that represent distinct sample areas of the different land cover types to be classified). With the unsupervised classification method, the software finds the spectral classes (or clusters) in the multi-band image without the investigator's intervention. Once the clusters are found, the investigator then needs to identify what each cluster represents (e.g., water, bare earth, vegetative cover, rocky outcrops, fossil localities, etc.). In this study we used a supervised classification model of the Uinta Basin and "trained" our polygons on six different land cover classes that we could identify from high-resolution satellite and/or aerial imagery (Bing Maps; RGB bands 7,5,1): 1) known fossil localities (those discovered prior to 2005); 2) oil/gas field infrastructure (graded well pads, access roads, pipelines, etc.); 3) water; 4) agricultural land; 5) scrub/tree cover; 6) steep slopes (based on Digital Elevation Models (DEM's) we created of the Uinta Basin) (Fig. 2). In supervised classification it is important to collect several training samples for each of the classes one wants to classify. After so doing, we then "merged" these individual training samples for each class using the Training Manager tool in ArcGIS®10 and gave each their own relevant name and color for display. We should emphasize that one of the strengths of these supervised classification methods is that they are very flexible and can be adapted to almost any region of paleontological interest. For example, researchers can identify any number of land cover classes relevant to particular geographical areas, in order to find the most promising "fossil locality" land cover classes in their own research areas. While fewer (or more) land cover classes might be appropriate in other geographical contexts, we found that, for the Uinta Basin, these six land cover classes provided the greatest clarity.

The next step in building our spectral analysis model was to create a signature file from the training samples of the six Uinta Basin land cover classes we had identified - a signature file records the spectral signatures of the different classes across a series of satellite bands. Once the distinct training samples had been identified and merged, and a signature file created, the image was classified using the maximum likelihood method for supervised classification within the spatial analysis toolkit of ArcGIS®10. Of course, cells in any given class are rarely homogeneous, therefore, the maximum likelihood method assigned each cell, or pixel, in the satellite image to one of our six different land cover classes based on the means and variances of the class signatures stored in the signature file. The algorithm used by the maximum likelihood classification tool is based on several assumptions:

- Each class should have a normal distribution in multivariate attribute space.
- The prior probabilities of the classes should be equal - that is, in the absence of any weighting of attribute values, all classes are equally likely. (If the prior probability is not equal for each class in a study area, one has the option of weighting the classes. This probability and weighting logic is based on Bayesian decision rules). The actual probability values for each cell and class are determined from the means and covariance matrix for each class stored in the signature file.

The maximum likelihood method considers both the variances and covariances of the class signatures when assigning each cell to one of the classes represented in the signature file. With the assumption that the distribution of a class sample is normal, a class can be characterized by the mean vector and the covariance matrix. Given these two characteristics for each cell value, the statistical probability is computed for each class to determine the membership of the cells to the class. Each cell is then assigned to the class to which it has the highest probability of belonging. Ultimately, the goal of maximum likelihood image classification is to assign each cell in the study area to a known class that has been "trained" by the investigator (supervised classification). This results in a map that partitions the study area into known classes that correspond to the spectral signatures of the training samples.

Class probability map

We further classified the Uinta Basin landscape by creating a class probability map. In this case, instead of having each cell assigned to a class based on the highest probability on an output raster, the class probability tool outputs a multi-band raster in which there is one band for each land cover class in the input signature file and each band stores the probability that a cell belongs to that class based on the attributes from the original input bands. In our model, we created a raster class probability map highlighting only those areas in the Uinta Basin having a >98% probability of having the same spectral signature as known (pre-2005) fossil bearing localities (shown in red in Fig. 3). To further refine our predictive model, we then executed an "extract by mask" function on this >98% probability raster (the "extract by mask" function essentially extracts the cells of a raster that correspond to the areas defined by a mask). The "mask" in this case was the geological map of the Uinta Basin showing only those areas mapped as Eocene. Thus, the resulting raster map shown (in red) in Fig. 3 highlights only those areas of the Uinta Basin that have both a >98% probability of falling within the land cover class "fossil localities" and are mapped as Eocene on the geological map of the Uinta Basin.

To review, the following are the steps we performed to create our "remote" prospecting model of the Uinta Basin:

1. Identify the relevant input bands (Landsat ETM+). See Table 1 for characteristics of each of these bands.

2. Create training samples (polygons) from known locations of desired classes. In our study, our training samples consisted of six land cover classes (Fig. 2):

- Known fossil localities (discovered prior to 2005)
- Oil/gas field infrastructure (graded well pads, access roads, pipelines, etc.)
- Water
- Agricultural cover
- Scrub/tree cover
- Steep slopes (based on Digital Elevation Models (DEM's) of the Uinta basin)

3. Create a signature file for the training samples.

4. Run the maximum likelihood classification

5. Create a class probability map (in our case, a map highlighting only those areas in the Uinta Basin having a >98% probability of having the same spectral signature as known (pre-2005) fossil bearing localities.

6. Run the “extract by mask” function using the >98% fossil localities land cover class as the input raster and the geological map of the Uinta Basin as the mask feature.

Results

A post-hoc validation of the spectral signature model

The results of our maximum likelihood classification and class probability models for the Uinta Basin are shown in Fig. 3. The yellow triangles are Washington University (WU) fossil localities discovered prior to 2005. These are the fossil localities that the image classification program was “trained” on to identify the land cover class “fossil localities”. Draped over the Uinta Basin base map (where some of the major drainages in the area are also labeled) is the class probability map – a single raster layer highlighting, in red, only those cells (pixels) within the Uinta Basin having both a >98% probability of being classified within the land cover class “fossil localities” and being mapped as Eocene on the geological map of the Uinta Basin.

After producing our maximum likelihood and class probability models of the Uinta Basin showing areas predicted to have a >98% chance of having fossiliferous sediments (based on the training sample of known fossil localities discovered prior to 2005), we needed some way to “ground truth” the model. A fortuitous “post-hoc” validation presented itself.

Prior to the creation of our Uinta Basin class probability model, we (meaning GC, CE, and RA) had no a priori knowledge whatsoever of whether or not any new fossil localities had been identified in the Uinta Basin since 2005. However, our model identified several paleontological "hotspots", regions that, while not producing any fossil localities prior to 2005, had high probabilities of being fossiliferous based on the similarities of their spectral signatures to those of previously known fossil localities (e.g., areas around Antelope Draw, Glen Bench, Lower Coyote Wash, and further to the west in the Uintah and Ouray Indian Reservation).

Subsequent to producing our Uinta Basin model, we (GC, CE, and RA) learned that fossil collecting had indeed continued in the Uinta Basin under the supervision of Beth Townsend and that 17 new fossil localities had been found since 2005. Without any knowledge of our class probability model (trained on pre-2005 fossil localities), she provided us with the GPS coordinates of her new fossil localities. Their locations are plotted in Fig. 3 (green dots). All of them fall within areas predicted by our model. Even though one site is located in the far southeastern part of the Basin near Upper Coyote Wash, quite removed from all other known fossil localities, it is still within a highly "predictable" region based on our model.

Regarding other predicted "hotspot" areas (for example, those areas near Glen Bench and Lower Coyote Wash), while few surface collections have been recovered thus far, consulting paleontologists are now reporting the discovery of numerous vertebrate fossils in these areas as a result of the excavation of well pads in the region. Because of these reports, paleontological collection strategies have now turned to excavation and screen washing in these regions. Unfortunately, the potentially fossiliferous areas predicted by our model to lie south and west of Johnson Bottom, Antelope Draw, and Glen Bench are not currently open to paleontological collecting since they are within either the Ouray National Wildlife Refuge or the Uintah and Ouray Indian Reservation. However, fossil localities are known to exist in these areas as well (KBT, pers. comm.).

Conclusions

Thus, without having a priori knowledge of any post-2005 fossil collecting activity within the Uinta Basin, our maximum likelihood and class probability models based on the spectral signatures of known (pre-2005) fossil localities have proven to be highly effective in informing paleontological explorations in this vast region. We believe that this relatively simple image classification model can be used to great advantage for paleontological explorations in almost any part of the world (Malakhov et al., 2009). By using the type of model we have presented here, combined, of course, with the relevant satellite imagery and land cover classifications, it

should now be possible for paleontologists to “remotely” prospect for fossils almost anywhere on earth – no matter how remote or expansive the area. The advantages are obvious. We suggest that such simple spectral signature modeling for “remote” fossil prospecting should become an important component in the armamentarium of paleontologists in the future.

Acknowledgments

From Washington University in St. Louis we thank A. Addison and W. Winston for GIS support and D.T. Rasmussen for sharing Uintan fossil locality data. We would also like to thank the Bureau of Land Management for permitting and logistical support in the Uinta Basin.

References

R. Anemone, G. Conroy, C. Emerson. GIS and Paleoanthropology: incorporating new approaches from the geospatial sciences in the analysis of primate and human evolution. Yrbk Phys. Anthropol., 54 (2011), pp. 19–46

R. Anemone, C. Emerson, G. Conroy. Finding fossils in new ways. Evol. Anthrop., 20 (2011), pp. 169–180

C. Betts. The Yale College expedition of 1870. Harper's New Monthly Mag. (1871), pp. 663–671

C. Black, M. Dawson. A review of late Eocene mammalian faunas from North America. Amer J. Sci., 264 (1966), pp. 321–349

B. Bryant, C. Naeser, R. Marvin, H. Mehnert. Upper Cretaceous and Paleogene sedimentary rocks and isotopic ages of Paleogene tuffs, Uinta Basin, Utah. US Geol. Surv. Bull., 1787 (1989), pp. j:1–j:22

T. Carr, M. Turner. Investigating regional lithic procurement using multi-spectral imagery and geophysical exploration. Archaeol. Prospect., 3 (1996), pp. 109–127

G. Conroy. Creating, displaying and querying interactive paleoanthropological maps using GIS: an example from the Uinta Basin, Utah. Evol. Anthrop., 15 (2006), pp. 217–223

G. Conroy, R. Anemone, J. Van Regenmorter, A. Addison. Google Earth, GIS, and the Great Divide: a new and simple method for sharing paleontological data. J. Hum. Evol., 55 (2008), pp. 751–755

E. Douglass. Geology of the Uinta formation. Geol. Soc. Amer. Bull., 25 (1914), pp. 417–420

C. Emerson, R. Anemone. An artificial neural network-based approach to identifying mammalian fossil localities in the Great Divide Basin, Wyoming. Remote Sensing Lett., 3 (5) (2012), pp. 453–460

M. Giardino. A history of NASA remote sensing contributions to archaeology. J. Archaeol Sci., 38 (2011), pp. 2003–2009

A. Hamblin, W. Sargeant, D. Spalding. Vertebrate Footprints in the Duchesne River and Uinta Formations (Middle to Late Eocene), Uinta Basin, Utah. Utah Geol Surv, Miscellaneous Publ (1999) pp. 443–454

K. Kvamme. Recent directions and developments in geographic informations systems. J. Archaeol Res., 7 (1999), pp. 153–201

D. Malakhov, G. Dyke, C. King. Remote sensing applied to paleontology: exploration of Upper Cretaceous sediments in Kazakhstan for potential fossil sites. Palaeontol. Electronica, 12 (2009), pp. 1–10

O. Marsh. Ancient lake basins of the Rocky Mountain region. Amer J. Sci. Arts, 4 (122–128) (1875), pp. 202–224

O. Marsh. Notice of new tertiary mammals, IV. Amer J. Sci. Arts, 9 (1875), pp. 239–250

M. McCoy, T. Ladefoged. New developments in the use of spatial technology in archaeology. J. Archaeol Res., 17 (2009), pp. 263–295

M. Mehrer, K. Westcott (Eds.), GIS and Archaeological Site Location Modeling, CRC Press, Boca Raton, Fl (2006)

P. Murphey, K. Townsend, A. Friscia, E. Evanoff. Paleontology and stratigraphy of middle Eocene rock units in the Bridger and Uinta basins, Wyoming and Utah. J. Lee, J. Evans (Eds.), Geologic Field Trips to the Basin and Range, Rocky Mountains, Snake River Plain, and Terranes of the US Cordillera, Geol. Soc. Amer. Field Guide (2011), pp. 125–166

K. Ostir, Z. Stancic, M. Trusnovec. Multispectral classification of satellite images. M. Gillings, D. Mattingly, J. van Dalen (Eds.), Geographical Information Systems and Landscape Archaeology. The Archaeology of Mediterranean Landscapes, Oxbow Books, Oxford (1999), pp. 125–132

S. Parcak. Satellite Remote Sensing for Archaeology. Routledge, New York (2009)

O. Peterson. Report upon the material discovered in the upper Eocene of the Uinta Basin by Earl Douglass in the years 1908–1909, and by O. A. Peterson in 1912. Ann. Carnegie Mus., 12 (1919), pp. 40–169

O. Peterson, J. Kay. The upper Uinta formation of northeastern Utah. Ann. Carnegie Mus., 20 (1931), pp. 293–306

D. Prothero. Magnetic stratigrapy and biostratigraphy of the Middle Eocene Uinta formation, Uinta Basin, Utah. D. Prothero, R. Emry (Eds.), The Terrestrial Eocene-Oligocene Transition in North America, Cambridge University Press, Cambridge (1996), pp. 3–24

D.T. Rasmussen, G.C. Conroy, A. Friscia, K. Townsend, M. Kinkel. Mammals of the Middle Eocene Uinta formation. D. Gillette (Ed.), Vertebrate Paleontology in Utah, Utah Geol. Soc., Salt Lake (1999), pp. 401–420

R. Ryder, T. Fouch, J. Elison. Early tertiary sedimentation in the western Uinta Basin, Utah. Geol. Soc. Amer., 87 (1976), pp. 496–512

W. Scott, H. Osborn. Preliminary report of the vertebrate fossils from the Uinta formation, collected by the Princeton expedition of 1886. Proc. Amer. Phil. Soc., 1887 (1887), pp. 255–264

W. Scott, H. Osborn. The Mammalia of the Uinta formation. Trans. Amer. Phil. Soc., 16 (1890), pp. 461–572

D. Sprinkel. Interim Geologic Map of the Vernal 30' by 60' Quadrangle, Uintah and Duchesne Counties, Utah, and Moffat and Rio Blanco Counties, Colorado. (2007) Utah State Geol. Surv. Map, OFR 506DM, scale 1:100,000

K.E. Townsend. Stratigraphy, Paleoecology, and Habitat Change in the Middle Eocene of North America. Ph.D. Dissertation, Washington University, St. Louis (2004)

K.E. Townsend, A.R. Friscia, D.T. Rasmussen. Stratigraphic distribution of Upper Middle Eocene fossil vertebrate localities in the Eastern Uinta basin, Utah, with comments on Uintan biostratigraphy. Mountain Geologist, 43 (2006), pp. 115–134

K.E. Townsend, D.T. Rasmussen, P.C. Murphey, E. Evanoff. Middle Eocene habitat shifts in the North American Western interior: a case study. Palaeogeo., Palaeoclim., Palaeoecol., 297 (2010), pp. 144–158

S. Walsh. Middle Eocene mammalian faunas of San Diego County, California. D. Prothero, R. Emry (Eds.), The Terrestrial Eocene-Oligocene Transition in North America, Cambridge University, Cambridge (1996), pp. 52–74

H. Wood, R. Chaney, J. Clark, E. Colbert, G. Jepsen, J. Reeside, C. Stock. Nomenclature and correlation of the North American continental tertiary. Geol. Soc. Amer. Bull., 52 (1941), pp. 1–48

M. Woodburne, G. Gunnell, R. Stucky. Land mammal faunas of North America rise and fall during the early Eocene. Denver Mus. Nat. Sci. Ann., 1 (2009), pp. 1–78

J. Zachos, M. Pagani, L. Sloan, E. Thomas, K. Billups. Trends, rhythms, and aberrations in global climate 65 Ma to present. Science, 292 (2001), pp. 686–693